ORIGINAL ARTICLE

Induction of tryptophan hydroxylase in the liver of s.c. tumor model of prostate cancer

Asami Hagiwara[1] [iD] | Yoshiyasu Nakamura[2] | Rumi Nishimoto[1] | Satoko Ueno[1] |
Yohei Miyagi[2]

[1]Material & Technology Solutions Labs, Research Institute for Bioscience Products & Fine Chemicals, Ajinomoto Co., Inc, Kawasaki City, Japan

[2]Molecular Pathology and Genetics Divisiosn, Kanagawa Cancer Center Research Institute, Kanagawa Cancer Center, Yokohama City, Japan

Correspondence
Yohei Miyagi, Kanagawa Cancer Center Research Institute, Kanagawa Cancer Center, Yokohama City, Japan.
Email: miyagi@gancen.asahi.yokohama.jp

Abstract

Enhanced degradation of tryptophan (Trp) and thus decreased plasma Trp levels are common in several types of cancers. Although it is well known that Trp catabolism is induced in the tumor microenvironment by the enzymes expressed in cancer cells, immune cells, or both, few studies have examined systemic Trp catabolism in cancer pathophysiology. The present study aimed to evaluate Trp catabolism in both tumor and peripheral tissues using tumor-engrafted Copenhagen rats that were s.c. inoculated with AT-2 rat prostate cancer cells negative for expression of Trp catabolic enzymes. Liquid chromatography-tandem mass spectrometry (LC-MS/MS) metabolomics showed significantly decreased plasma Trp levels in AT-2 engrafted rats, accompanied by increased kynurenine/Trp ratios in spleen and thymus and serotonin levels in liver and thymus. Quantitative PCR and enzymatic activity assays showed indoleamine-2, 3-dioxygenase, an inducible enzyme that catalyzes Trp to kynurenine, was increased in tumor tissues, whereas tryptophan-2,3-dioxygenase, a major Trp catabolic enzyme that regulates systemic level of Trp, tended to be increased in the liver of AT-2 engrafted rats. Furthermore, tryptophan hydroxylase-1 (TPH1), an enzyme that catalyzes the reaction of Trp to serotonin, was significantly increased in liver and spleen of AT-2 engrafted rats. Further histochemical analysis revealed that the induction of TPH1 in the liver could be attributed to infiltration of mast cells. A similar phenomenon was observed with nonneoplastic liver samples from colorectal cancer patients. These results suggested that Trp catabolism toward serotonin synthesis might be induced in peripheral remote tissues in cancer, which could have a pathophysiological effect on cancer.

KEYWORDS
liver, mast cell, serotonin, tryptophan, tryptophan hydroxylase

---

1 | INTRODUCTION

Enhanced tryptophan (Trp) catabolism is associated with various health conditions including aging, infection, neurodegenerative disorders, and cancers.[1] Because Trp catabolism generates many important biologically active metabolites involved in diverse physiological functions, including inflammation, immune response, and neurotransmission, enhanced Trp catabolism could be a direct cause for various pathological conditions.[2] Thus, it is important to investigate its underlying mechanisms in distinct pathological contexts to understand each pathology and to develop therapeutic interventions to prevent and treat them.

Tryptophan is catabolized mainly by two pathways, the oxidative Trp-Kyn pathway and the hydroxylation Trp-serotonin (5-hydroxytryptamine) pathway[3] (Figure 1). The Trp-Kyn pathway accounts for the majority (~95%) of dietary Trp disposal. The metabolites produced in this pathway include the immune suppressive metabolite Kyn, the important redox cofactor NAD, N-methyl-D-aspartate receptor antagonist kynurenic acid, and the antagonist quinolinic acid. The rate-limiting first step of the Trp-Kyn pathway is mediated by 2 enzymes, tryptphan-2, 3-dioxygenase (TDO) and indoleamine-2, 3-dioxygenase (IDO). TDO is constitutively expressed at high levels in the liver and is responsible for the regulation of systemic levels of Trp. IDO is mostly expressed in immune cells and its activity is negligible under basal conditions, but is greatly induced by inflammatory mediators such as IFN-γ. The Trp-serotonin pathway is initiated by the rate-limiting enzyme tryptphan hydroxylase (TPH) that exists in 2 isoforms, TPH1 and TPH2. TPH1 is mainly expressed in the gut, and TPH2 is in neurons.

Recently, Trp catabolism through the Trp-Kyn pathway in cancer has received increasing attention because it contributes to the suppression of antitumor immune response.[4] It has been proposed that Trp is actively catabolized in tumor tissue by both cancer cells and tumor-infiltrating immune cells. The local Trp depletion and subsequent accumulation of immunosuppressive Trp metabolites in the tumor microenvironment lead to T cell anergy and apoptosis, thus suppressing antitumor immune response and promoting tumor growth.[5]
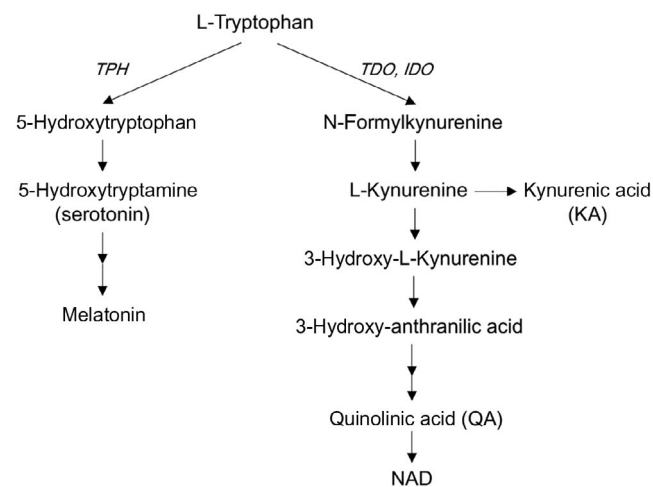

FIGURE 1 Tryptophan metabolism along kynurenine and serotonin pathways. IDO, indoleamine-2, 3-dioxygenase; TDO, tryptophan-2, 3-dioxygenase; TPH, tryptophan hydroxylase

Several clinical studies have shown that low levels of serum/plasma Trp and/or elevated levels of its metabolite Kyn, both of which result in an increased Kyn/Trp ratio, can be used as indicators of enhanced Trp catabolism in several types of cancers, including T-cell leukemia,[6] lung cancer,[7] melanoma,[8] gynecological cancer,[9] and colorectal carcinoma.[10,11] We have also reported that low plasma Trp level is common among the 5 different types of cancer patients.[12] The elevated systemic Kyn/Trp ratio can be attributed to not only Trp catabolism in the tumor microenvironment but also systemic Trp catabolism. Despite considerable advances in our understanding of Trp catabolism in the tumor microenvironment, little is known about systemic activation of Trp catabolism in cancer physiology. Although the close relationship between Kyn/Trp ratio and immune activation markers, such as neopterin and C-reactive protein, in serum/plasma is known as an indicator of systemic IDO activation by IFN-γ,[13] other possibilities, such as activation of Trp catabolism by TDO and/or through the Trp-serotonin pathway, have not been investigated.

Here, using a tumor animal model engrafted with autologous prostate cancer cells deficient for TDO, IDO, and TPH, we show that Trp catabolic enzymes are induced both in tumor tissue and remote tissues, especially in the liver. The present results suggest that Trp catabolism, not only in the tumor microenvironment but also in peripheral remote tissues, might be responsible for enhanced Trp catabolism in cancers.

2 | MATERIALS AND METHODS

2.1 | Cell line

The AT-2 rat prostate cancer cell line is one of the cell lines established from the Dunning R3327 prostate adenocarcinoma that spontaneously arose in a male Copenhagen rat.[14] AT-2 cells have relatively low metastatic ability compared with other highly metastatic sublines established from the same tumor.[15] This cell line was a generous gift from the original founders through Hisao Ekimoto, PhD, at the Oncology Section, Laboratory of Biology, Nippon Kayaku Co., Ltd., and was maintained at the Kanagawa Cancer Center. AT-2 cells were grown in RPMI-1640 medium (Thermo Fisher Scientific) supplemented with 10% FBS at 37°C under humidified room air with 5% CO_2. Cells were generally passaged 3 times for amplification before engraftment.

2.2 | Tumor engrafted model

Male Copenhagen rats were purchased from the Institute for Animal Reproduction. For the autologous rat prostate cancer model, 5×10^6 AT-2 cells were inoculated in the back of a male Copenhagen rat, and the grown tumor autograft was obtained when it measured 15 mm in the largest diameter. The tumor was then dissected into cubes of 3 mm per side and subsequently engrafted in the back of 6 male Copenhagen rats (7 weeks of age). Skin incisions were also made on 6 control rats without engraftment of tumors as the sham operation. All surgical

procedures were carried out under inhalational anesthesia with isoflurane. The Kanagawa Cancer Center Animal Care and Use Committee approved this experiment under protocol 28-02.

2.3 | Sample collection

Blood samples were collected from tail veins of rats at 0, 1, 2, 3, and 4 weeks of tumor engraftment. At 5 weeks of engraftment, the rats were anesthetized with isoflurane after 6 hours of starvation and blood was collected from the inferior vena cava. After the rats were killed by exsanguination, whole tissues were collected immediately and rinsed with ice-cold saline. A part of each tissue was fixed in 10% neutral buffered formalin. The remnant tissues were snap frozen in liquid nitrogen. Blood samples were mixed with EDTA and kept on ice until plasma collection by centrifugation. All samples were stored at −80°C. All frozen tissue samples were crushed by a Multi-Beads Shocker (Yasui Kikai) to make homogenous powder before proceeding to subsequent analysis.

2.4 | Metabolites analysis

Frozen tissue samples were homogenized with a 50-times volume of 80% methanol supplemented with 1% Phe-d5 as an internal control. The homogenates were extracted with chloroform, and aqueous fractions were dried. The samples were reconstituted in a tenth volume of water. Plasma samples were deproteinized with acetonitrile. The extracted tissue samples and deproteinized plasma samples were derived with 3-aminopyridyl-N-hydroxysuccinimidyl carbamate before LC-MS/MS analysis as previously described.[16] Tryptophan was analyzed and quantified using LC-MS/MS (Agilent 1290 Infinity series liquid chromatography system; Agilent Technologies) coupled to an API4000 mass spectrometer (AB Sciex). Kynurenine, 5-HTP, and serotonin were analyzed and quantified using LC-MS/MS (ACQUITY UPLC system; Waters) coupled to a 5500 QTRAP mass spectrometer (AB Sciex) as described previously.[17]

2.5 | RNA isolation and qPCR

Total RNA was extracted from tissues by using the RNeasy plus universal kit (Qiagen) according to the manufacturer's protocol. cDNA was synthesized from 1 μg RNA with a High-Capacity cDNA Reverse Transcription Kit (Thermo Fisher Scientific). Real-time qPCR was undertaken using the power SYBR Green PCR Master Mix (Thermo Fisher Scientific) and quantified using StepOne Plus Real-Time PCR systems (Thermo Fisher Scientific). Relative quantitation of gene expression was determined by using the comparative CT (ΔΔCT) method and normalized to *β-actin*. For *Ido1*, the RT^2 qPCR Primer set for Rat *Ido1* (Qiagen) was used. For others, custom-made primers were used. The sequences for the primer pairs were as follows *Tdo2* forward, 5′-GGC TAT TAT TAT CTG CGC TCA ACT G -3′ and reverse

5′-GAA CCA GGT ACG ATG AGA GGT TAA A-3′; *Tph1* forward, 5′-CAA GGA GAA CAA AGA CCA TTC −3′ and reverse, 5′- ATT CAG CTG TTC TCG GTT GAT G −3′; and *β-actin* forward, 5′- GCA GGA GTA CGA TGA GTC CG −3′ and reverse, 5′- ACG CAG CTC AGT AAC AGT CC −3′.

2.6 | Western blot analysis

Tissues were homogenized in RIPA buffer (Nacalai Tesque) supplemented with protease inhibitor cocktail (Nacalai Tesque). Protein concentrations were measured by bicinchoninic acid assay (Thermo Fischer Scientific), and 30 μg protein was loaded per lane and separated by SDS-PAGE electrophoresis, followed by trans blotting to PVDF membranes. The membranes were blocked with StartingBlock (PBS) Blocking Buffer (Thermo Fischer Scientific) and immunoblotted overnight with either anti-TDO2 polyclonal Ab (#MBS9133230; MyBioSource) or anti-β-actin Ab (#CST4967; Cell Signaling Technology). The immobilized Ab was detected using the HRP-conjugated secondary Ab (Cell Signaling Technology) and Chemi-Lumi One Super (Nacalai). The images were visualized by Amersham Imager 600 (GE Healthcare).

2.7 | Tryptophan-2,3-dioxygenase activity assay

Tryptophan-2,3-dioxygenase activity assay was carried out according to the method described by Gibney et al[18] with minor modifications. Briefly, 50 mg tissue was homogenized in 0.5 mL PBS supplemented with protease inhibitor cocktail (Nacalai Tesque). Homogenates were centrifuged at 10 000 *g* for 10 minutes. A 0.1 mL aliquot of the supernatant was mixed with an equal volume of reaction mixture containing 50 mmol/L sodium phosphate buffer (pH 7.0), 2 μmol/L hematin, and 800 μmol/L L-Trp at final concentrations. The solution was incubated at 37°C with 300 rpm shaking. After 60 minutes, the reaction was stopped by the addition of trichloroacetic acid (90 mmol/L final concentration) followed by heating at 65°C for 15 minutes to hydrolyze N-formylkynurenine to Kyn. The solution was centrifuged at 20 000 *g* for 5 minutes, and 100 μL supernatant was mixed with an equal amount of Ehrlich's reagent in a 96-well microtiter plate. The absorbance was measured at 480 nm. Kynurenine concentrations in each sample were calculated from a standard curve of defined concentrations of Kyn. The TDO activity of each sample was reported as picomole of Kyn produced per microgram of protein. All samples were measured in triplicate and inactivated samples (by adding trichloroacetic acid before reaction) were used as negative controls in each assay.

2.8 | Indoleamine-2, 3-dioxygenase-1 activity assay

Tissue homogenates were prepared as described above. A 0.2 mL aliquot of the supernatant was mixed with an equal volume of reaction mixture containing 50 mmol/L potassium phosphate buffer (pH 6.5),

20 mmol/L ascorbate, 10 µmol/L methylene blue, 100 µg/mL catalase, and 400 µmol/L L-Trp at final concentrations. The solution was incubated at 37°C for 30 minutes, then the reaction was stopped by the addition of 20 µL trichloroacetic acid (90 mmol/L final concentration). The following procedures were performed the same as TDO activity assay. IDO activity of each sample was reported as picomole of Kyn produced per microgram of protein. All samples were measured in duplicate and inactivated samples (by adding trichloroacetic acid before reaction) were used as negative controls in each assay.

2.9 | Tryptophan hydroxylase-1 activity assay

Tryptophan hydroxylase-1 activity assay was carried out using a modification of the method described by Kuhn et al.[19] Briefly, 50 mg tissue was homogenized in 0.5 mL of 50 mmol/L Tris-HCl (pH 7.4) containing 2 mmol/L DTT supplemented with protease inhibitor cocktail (Nacalai Tesque). Homogenates were centrifuged at 20 000 g for 20 minutes. A 10 µL aliquot of the supernatant was mixed with 90 µL reaction mixture containing 50 mmol/L Tris-HCl (pH 7.4), 8 IU/µL catalase, 0.4 mmol/L L-Trp, and 0.5 mmol/L 6-MPH4 at final concentrations. The solution was mixed and incubated at 37°C for 15 minutes. The reaction was stopped by adding 20 µL of 6 N perchloric acid. The solution was centrifuged at 20 000 g for 20 minutes. Then 40 µL supernatant was mixed with 100 µL of 8 N HCl in a 96-well microtiter plate. The fluorescence of the solution was measured by Varioskan LUX (Thermo Fisher Scientific) at excitation-emission wavelengths of 295/345 nm. The amount of 5-HTP formed enzymatically was calculated from a standard curve of defined concentration carried through the entire procedure. The TPH1 activity of each sample was reported as picomole of 5-HTP produced per microgram of protein. All samples were measured in triplicate in each assay and inactivated samples (by heat inactivation before reaction) were used as negative controls in each assay.

2.10 | Quantification of NADPH

Quantification of NADPH in the liver was carried out by using the NADP/NADPH quantification colorimetric kit (BioVision) according to the manufacturer's protocol.

2.11 | Immunohistochemical staining

Formalin-fixed tissues were embedded in paraffin, and thin 4 µm sections were prepared for immunohistochemistry. The antigen was retrieved by incubating in citrate buffer (pH 6.0) in a steamer. Endogenous peroxidase activity and nonspecific Ab binding were blocked with 3% hydrogen peroxide and with a blocking reagent (Biocare Medical), respectively. A rabbit mAb raised against a synthetic peptide corresponding to residues near the C-terminus of human TPH (EP1311Y; Abcam) was applied at a 1:50 dilution of the supplied hybridoma culture supernatant. Immunoreactivity was visualized by the

peroxidase-labeled amino acid polymer method with the MAX-PO Histofine simple stain kit (Nichirei) according to the manufacturer's instructions. The slides were analyzed by a BX53 Upright Microscope (Olympus) and images were captured by a DP21 system (Olympus).

2.12 | In situ hybridization

Thin sliced formalin-fixed tissue sections were prepared as described for immunohistochemistry. In situ hybridization was carried out by the RNAscope (ACD) assay system with either a custom-made probe targeting rat _Tph1_ mRNA (#52673; ACD) or a scramble probe as a negative control, and RNAscope 2.5 HD Detection Reagent-RED (ACD) precisely following the manufacturer's instructions.

2.13 | Toluidine blue staining

Toluidine blue staining of paraffin-embedded liver samples was undertaken by Biopathology Institute Co., Ltd.

2.14 | Immunohistochemistry for liver of tumor burden patients

The FFPE nonneoplastic liver tissues of tumor burden patients were prepared from the archives of the Pathology Department of Kanagawa Cancer Center. For this purpose, we screened the pathology record and selected 10 patients who received surgical removal of liver metastasis with simultaneous resection of the primary colorectal cancer. The FFPE sections for IHC were prepared from the nonneoplastic background liver of the partial hepatectomy specimens of metastatic colorectal cancer. Written broad informed consent for future use of specimens for research was obtained from each patient. This study was approved by the Research Ethics Committee of Kanagawa Cancer Center under the protocol EPI-113-2018. A control non-neoplastic liver FFPE specimen was purchased from Zyagen.

2.15 | Statistical analysis

Student's unpaired t test was used to determine differences between 2 groups (N = 6 per group). Significance was judged when P values were less than .05. Statistical analysis was carried out with GraphPad Prism 6.0 (GraphPad Software).

3 | RESULTS

3.1 | Tryptophan, kynurenine, and 5-HTP levels in plasma

We quantified plasma levels of Trp, Kyn, and 5-HTP, the immediate precursor of serotonin (Figure 1), before and 1, 2, 3, 4, and 5 weeks

after tumor cell inoculation. Plasma Trp levels in controls were stable and maintained at approximately 120 μmol/L during the study period. In contrast, plasma Trp levels in the AT-2 engrafted model started to decline from 1 week after the engraftment, and after 5 weeks, it was decreased by 42% (Figure 2A). Plasma Kyn (Figure 2B) and 5- HTP (Figure 2C) levels tended to be lower in AT-2 engrafted rats compared to control, but did not reach statistical significance at any time point. The Kyn / Trp ratio showed a trend to increase and 5-HTP / Trp ratio increased significantly in AT-2 engrafted rats compared to control (Figure 2D,E).

3.2 | Tryptophan, kynurenine, and serotonin levels in tissues

We next quantified levels of Trp, Kyn, and serotonin in several tissues, including liver, small intestine (jejunum and ileum), immune tissues (spleen and thymus), and tumor. As shown in Table 1, at 5 weeks after tumor cell inoculation, the Trp level was significantly decreased in spleen, while the Kyn level was significantly increased in thymus of AT-2 engrafted rats. The Kyn / Trp ratio was significantly increased in spleen and thymus of AT-2 engrafted rats. Surprisingly, serotonin levels in liver and thymus were increased in AT-2 engrafted rats, and the magnitude of increase in liver was 5-fold.

3.3 | Tryptophan-2, 3-dioxygenase activity tends to be increased in liver and tumor tissues of AT-2 engrafted rats

To examine the Trp-Kyn pathway, we first measured mRNA, protein, and enzymatic activity levels of hepatic TDO, the rate-limiting enzyme responsible for regulating systemic Trp levels. Although there were no differences in the levels of TDO mRNA (Figure 3A and Table S1) and protein (Figure 3B) between control and AT-2 engrafted rats, there was a trend of increased enzymatic activity in AT-2 engrafted rats compared to control (Figure 3C,
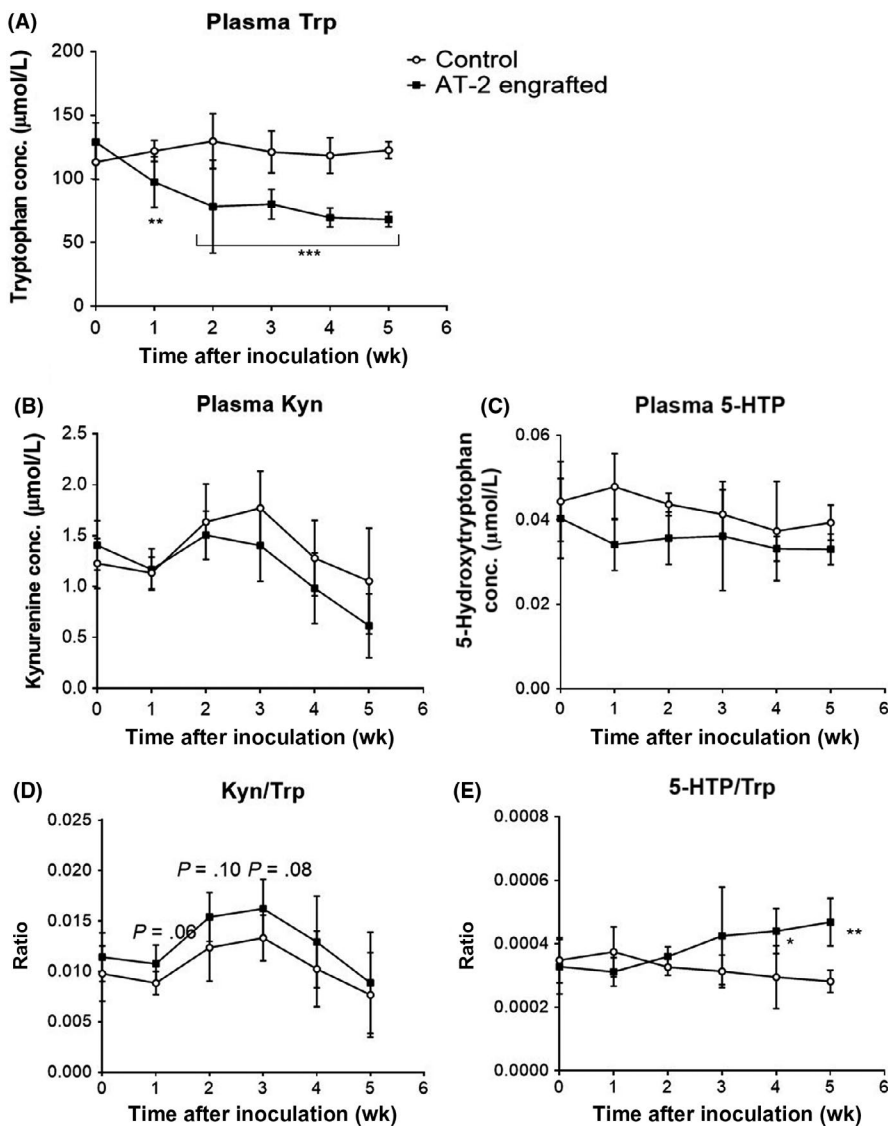

FIGURE 2 Tryptophan (Trp) and its metabolite concentrations (conc.) in plasma. Plasma Trp (A), kynurenine (Kyn) (B), and 5-hydroxytryptophan (5-HTP) (C) concentrations, and Kyn / Trp (D) and 5-HTP / Trp (E) ratios in control and AT-2 engrafted rats were measured every week after tumor inoculation for 5 weeks. Data are the means ± SD (N = 6/group). *P < .05, **P < .01, ***P < .001 vs control by Student's t test

TABLE 1 Tryptophan (Trp), kynurenine (Kyn), and serotonin concentrations (pmol/mg tissue) and Kyn / Trp ratio in tissues

	Trp			Kyn			Kyn / Trp			Serotonin		
	Control	AT-2 engrafted	P value	Control	AT-2 engrafted	P value	Control	AT-2 engrafted	P value	Control	AT-2 engrafted	P value
Liver	74.3 ± 7.6	73.0 ± 4.6	.88	1.1 ± 0.1	1.3 ± 0.2	.44	0.014 ± 0.001	0.018 ± 0.003	.15	4.3 ± 0.4	22.7 ± 6.1	<.05
Jejunum	101.0 ± 18.6	106.2 ± 34.3	.90	0.7 ± 0.1	0.8 ± 0.2	.63	0.009 ± 0.002	0.011 ± 0.004	.59	26.1 ± 3.7	23.8 ± 1.9	.59
Ileum	128.4 ± 25.5	124.4 ± 34.0	.93	2.1 ± 0.6	1.7 ± 0.3	.55	0.022 ± 0.011	0.021 ± 0.007	.95	33.0 ± 4.0	25.3 ± 3.1	.16
Spleen	106.7 ± 6.8	80.0 ± 4.6	<.05	0.7 ± 0.1	0.8 ± 0.1	.51	0.007 ± 0.001	0.011 ± 0.001	<.05	20.5 ± 0.8	14.3 ± 3.8	.14
Thymus	52.0 ± 1.3	52.8 ± 2.4	.79	1.5 ± 0.2	4.1 ± 0.7	<.01	0.028 ± 0.004	0.078 ± 0.011	<.01	8.0 ± 0.6	19.8 ± 1.4	<.01
Tumor		64.6 ± 4.5			4.1 ± 2.4			0.060 ± 0.031			7.2 ± 1.2	

Note: Data are the means ± SD (N = 6 per group).

P values indicate the significance of *t* tests between control and AT-2 engrafted rats.
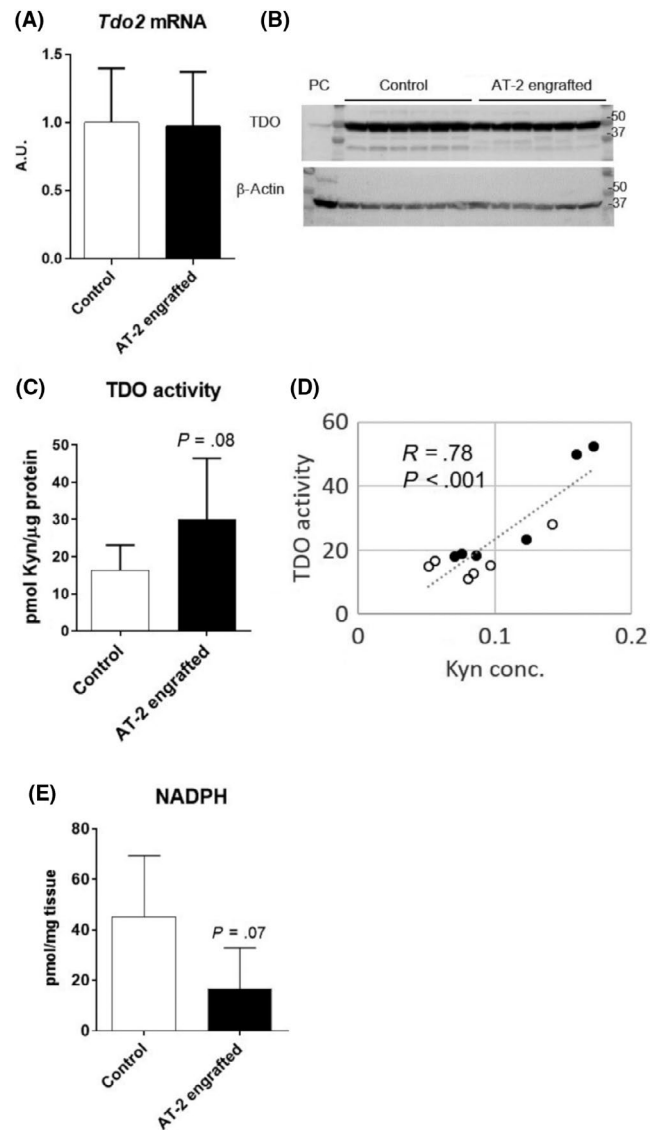

FIGURE 3 Tryptophan-2, 3-dioxygenase (TDO) activities tend to be increased in livers of AT-2 engrafted rats. A, B, mRNA (A) and protein levels of TDO2 (B) in the liver after 5 weeks of tumor inoculation. C, TDO activities in the liver. D, Correlation between TDO activities and kynurenine concentration (Kyn conc.) in liver. Pearson's correlation coefficient (R) and *P* values are reported. E, NADPH levels in liver. PC, Positive control (HepG2 cell homogenates)

Table S2). The livers with increased hepatic TDO activities showed higher levels of intrahepatic Kyn, and they were well correlated with each other (Figure 3D). As it has been reported that TDO is allosterically inhibited by NADPH,[20] we measured NADPH levels in the liver. There was a trend of decrease in the level of NADPH in the liver of AT-2 engrafted rats compared to control (Figure 3E). These results suggested that TDO activities in some of the livers of AT-2 engrafted rats were higher than control, most likely due to reduced inhibition by NADPH.

We then measured *Ido1* mRNA levels in immune tissues, ie, spleen and thymus, as they showed increased Kyn / Trp ratios as described above (Table 1), and also in tumor. Despite increased Kyn / Trp ratios

in immune tissues, *Ido1* mRNA levels were significantly decreased in AT-2 engrafted rats (Figure 4, Table S1). The IDO enzymatic activity showed high variation among the samples but the average was similar between control and AT-2 engrafted rats (Figure 4, Table S2). (We could not evaluate IDO activity in thymus due to the limited number of tissue samples.) Notably, tumor tissue showed relatively high IDO1 activity when compared with spleen (Figure 4, Table S2). The result showed that IDO1 was active in the tumor microenvironment, most likely by infiltration of IDO1-expressing immune cells.

3.4 | Tryptophan hydroxylase-1 is greatly increased in liver and spleen of AT-2 engrafted rats

Tryptophan hydroxylase is a rate-limiting enzyme that catalyzes the first step of the Trp catabolic pathway that produces serotonin and melatonin. The majority of peripheral TPH1 is expressed in the small intestine. We observed that the mRNA level of *Tph1* was highest in ileum and jejunum among the investigated tissues (Figure 5A, Table S1). To our surprise, *Tph1* mRNA level in the liver of AT-2 engrafted rats were similar as in the small intestine, whereas it was not detectable in the liver of control rats. Additionally, *Tph1* mRNA levels in spleen were greatly increased (8.8-fold) in AT-2 engrafted rats. We confirmed that TPH1 enzymatic activities were significantly increased in these tissues of AT-2 engrafted rats (Figure 5B, Table S2). Additionally, tumor tissue of AT-2 engrafted rats showed significant levels of *Tph1* mRNA expression and TPH1 enzymatic activities (Figure 5A,B, Tables S1 and S2). These results showed TPH1 was upregulated not only in tumor but also in peripheral remote tissues, liver and spleen, in AT-2 engrafted rats.

As few studies have reported TPH1 expression in the liver, and this was the first evidence, to our knowledge, to show upregulation of TPH1 in the liver, we decided to examine this observation more in detail. Immunohistochemical staining (Figure 5C) and in situ hybridization (Figure 5D) of TPH1 showed that the TPH1-positive cells were sparsely distributed in hepatic lobules and
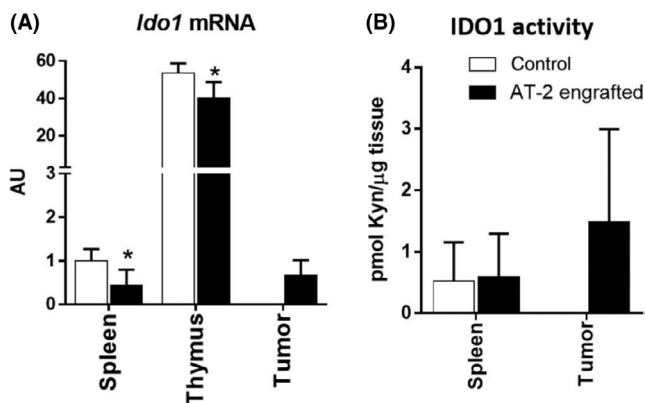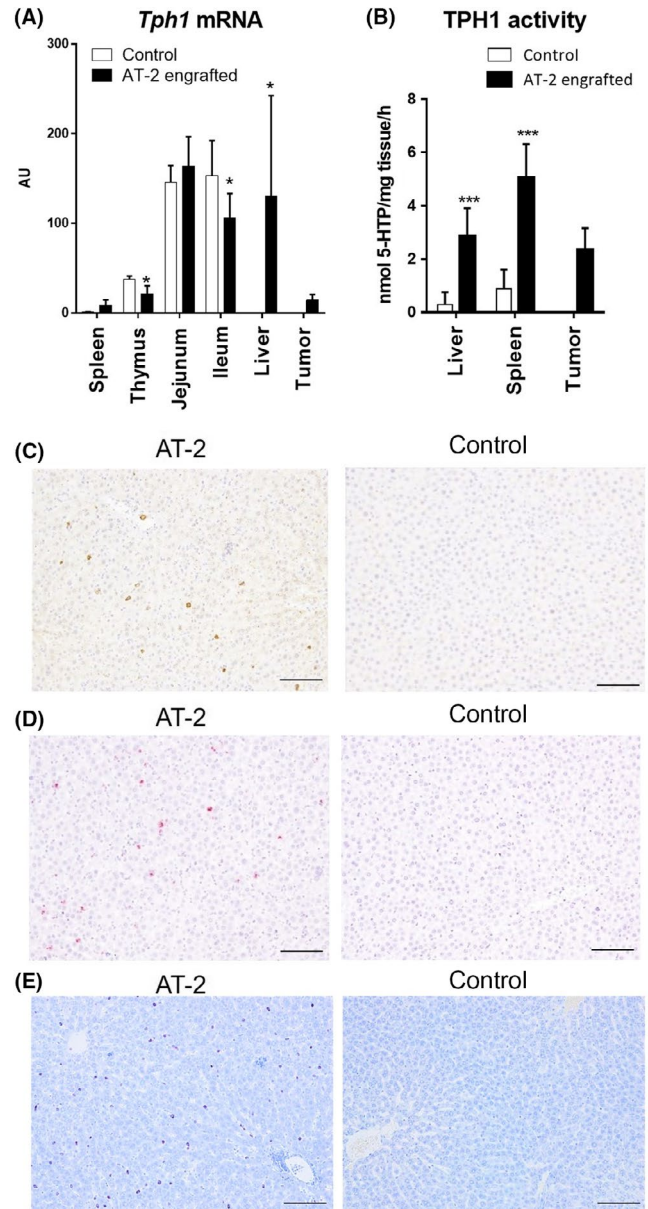

FIGURE 5 Tryptophan hydroxylase-1 (TPH1) expression and activity are significantly increased in liver and spleen of AT-2 engrafted rats. A, *Tph1* mRNA levels in investigated tissues. Results were normalized to the level in spleen of control that showed lowest expression. Data are means ± SD (N = 6/group). *$P < .05$, **$P < .01$ vs control by Student's *t* test. B, TPH1 activities in liver, spleen, and tumor. Data are means ± SD (N = 6/group). ***$P < .001$ vs control by Student's *t* test. C, Representative images of immunohistochemical staining of TPH1 in livers of control and AT-2 rats. Brown staining indicates TPH1 protein. D, Representative images of in situ hybridization of TPH1 in livers of control and AT-2 rats. Red staining indicates TPH1 expression. E, Representative images of toluidine blue staining of livers of control and AT-2 rats. Red purple staining indicates the presence of mast cells. Scale bar = 100 μm

FIGURE 4 Indoleamine-2, 3-dioxygenase-1 (IDO1) is induced in tumor but not in immune tissues of AT-2 engrafted rats. A, mRNA levels of *Ido1* in spleen, thymus, and tumor. B, IDO1 activities in spleen and tumor. Data are means ± SD (N = 6/group). *$P < .05$, calculated by Student's *t* test. Kyn, kynurenine

reside in the sinusoids in the livers of AT-2 engrafted rats. From these histologic observations, we speculated that these cells appear to originate from immune cells, as monocytes/macrophages, mast cells, and T cells are known to express TPH1.[21] Among these

FIGURE 6 Tryptophan hydroxylase-1 (TPH1)-positive cell infiltration into nonneoplastic livers of colorectal cancer (CRC) patients. Representative images of TPH1 immunohistochemical staining in the livers of 2 CRC patients and a healthy subject. Arrowheads in top panels indicate TPH1-positive cells. Scale bar = 100 μm
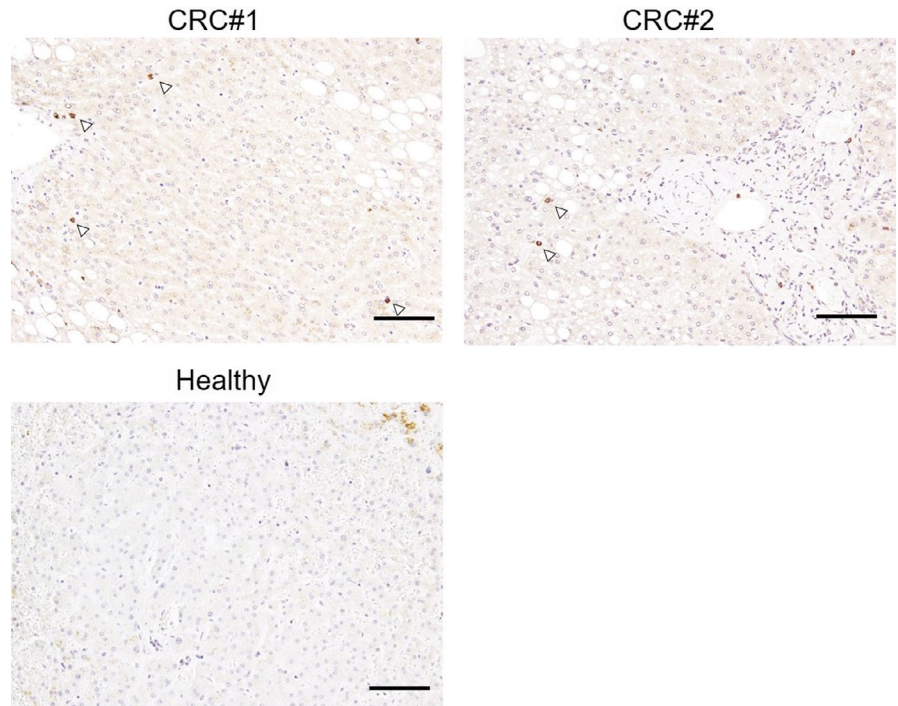
cells, mast cells were the most likely candidates, as we observed a high correlation between the levels of intrahepatic serotonin and histamine (Figure S1). Increased infiltration of mast cells in the livers of AT-2 engrafted models was confirmed by toluidine blue staining (Figure 5E). Although red-purple staining was rarely observed in control livers, it was increased in AT-2 engrafted models, and the staining pattern was similar to that of TPH1 staining. From these observations, we conclude that serotonergic TPH1 was upregulated in the liver of the AT-2 engrafted model, most likely due to increased infiltration of mast cells.

3.5 | Tryptophan hydroxylase-1-positive cells infiltration observed in remote liver tissues of colorectal cancer patients

To examine the physiological relevance of the above findings, we undertook TPH1 immunohistochemical staining on nonneoplastic liver tissues of tumor burden patients who received simultaneous surgical resection of primary colorectal cancer and liver metastasis. Two of 10 nonneoplastic background liver tissues examined revealed the same findings to the animal experiments, containing sparsely infiltrating TPH1-positive cells. Control liver tissue did not contain such cells (Figure 6).

4 | DISCUSSION

In the present study, to understand the mechanisms underlying the decreased systemic level of Trp in cancers, we investigated Trp catabolic enzymes in the tumor burden animal model, focusing on both tumor

and peripheral remote tissues. We showed that both IDO1 and TPH1 were expressed and active in tumor tissues, although the prostate cancer AT-2 cells used in this study were negative for expression of these genes when analyzed by qPCR (data not shown). This suggests that Trp is catabolized in the tumor microenvironment, most likely by resident immune cells that express IDO1 and/or TPH1. In addition, we found that TDO and TPH1 were upregulated in peripheral remote tissues, liver and spleen, of AT-2 engrafted rats (Figure S2).

The most striking difference in peripheral remote tissues was an induction of TPH1 and elevated level of serotonin observed in the liver of AT-2 engrafted rats, which was most likely caused by mast cell infiltration into the tissue. Furthermore, the TPH1 induction in the liver was also observed in some of the clinical samples from colorectal cancer patients who received simultaneous surgical resection of primary colorectal cancer and liver metastasis. We speculate that these findings suggest a possibility of enhanced local Trp catabolism toward serotonin, as similar observations have been reported with pulmonary arterial hypertension model rats induced by monocrotaline that have increased mast cell accumulation, TPH1, and serotonin levels in the lung, all of which were inhibited by TPH1 inhibitors.[22] We also observed a trend of upregulation of hepatic TDO activity in the liver of AT-2 engrafted rats, which was likely attributed to decreased levels of NADPH, an allosteric inhibitor of TDO in the tissue. Intrahepatic Trp catabolism is affected not only by activities of Trp catabolic enzymes but also other factors including intratissue Trp and plasma free Trp levels.[23] Intrahepatic Trp levels were similar (Table 1), but we assume plasma free Trp levels were increased in AT-2 engrafted rats as they showed lower albumin and higher NEFA levels relative to control rats (Figure S3), both of which increase free Trp.[23] Although additional experiments with isotope tracer to validate the net local Trp catabolism in the liver are required, our study was the first to show the possibility

that Trp catabolism toward both serotonin and Kyn pathways could be induced not only in the tumor microenvironment but also in the remote tissues with tumor burden model.

It remains to be seen to what extent the observed TPH1 and TDO induction in the liver accounts for the reduced steady-state level of plasma Trp in AT-2 engrafted rats. As it is widely accepted that induction of hepatic TDO activity leads to proportionate decreases in circulating Trp level,[24] the observed induction of hepatic TDO activity in some of the AT-2 engrafted rats could be one of the reasons for the reduced plasma Trp level in these animals. We hypothesize that the TPH1 induction in the liver of AT-2 engrafted rats could also account for the reduced circulating Trp level of these animals, to some extent, by the following 2 reasons. First, the mRNA level of TPH1 in the liver of the AT-2 engrafted model was comparable to those in the small intestine (jejunum and ileum, Figure 5A), where normally more than 90% of TPH1 is expressed. Second, it has been shown that deletion of peripheral TPH1 resulted in the significant increase in the steady-state levels of serum Trp in TPH1-knockout mice,[25] suggesting that peripheral TPH1 accounts for the systemic level of Trp. As the liver has a large organ mass, the significant TPH1 induction in this tissue, to a similar extent as in small intestine, might have an impact on systemic steady-state levels of Trp.

The induction of TPH1 in the liver of the AT-2 engrafted model was most likely due to the infiltration of mast cells into the tissue, as TPH1 IHC staining and toluidine blue staining were similar. Mast cells can reside in almost all the major tissues of the body, including the liver. Hepatic mast cells have been shown to increase in patients with several liver diseases, including primary biliary cirrhosis, primary sclerosis cholangitis, and hepatocellular carcinoma.[26] There are several studies suggesting that hepatic mast cells are involved in the pathological response to chronic inflammation, fibrogenesis,[27,28] and angiogenesis.[29] Although it is unknown whether the liver of the AT-2 engrafted model is damaged or has inflammation, we sometimes observed hepatic metastasis when they were kept more than 8 weeks after tumor inoculation on the back. Thus, it might be possible that mast cells infiltrated into the liver of the AT-2 engrafted model and created an immunosuppressive microenvironment, which eventually promoted cancer cell metastasis into the tissue.

There are several limitations in this study. First, we used only AT-2 engrafted rats as model animals and did not examine reproducibility of our findings with other models. Second, we did not show a direct relationship between the induction of Trp catabolic enzymes in peripheral remote tissues and the reduced level of plasma Trp.

In summary, we proposed a possibility that Trp catabolism in a tumor engrafted model was increased not only in the tumor microenvironment but also in the peripheral tissues, especially in the liver, by upregulation of TPH1 and TDO. Tryptophan catabolism by IDO and TDO by both immune and cancer cells in the tumor microenvironment have been investigated in numerous studies, whereas Trp catabolism in remote tissues has not received so much attention. Our findings suggest that the Trp catabolism in remote peripheral tissues should also be taken into consideration in understanding the pathophysiology and the management of cancer.

DISCLOSURE

AH, RN, and SU are employees of Ajinomoto Co., Inc. YN and YM declare that they have no conflict of interest.

ETHICS APPROVAL AND CONSENT TO PARTICIPATE

Experiments using tissue samples from human subjects were approved by the Research Ethics Committee of Kanagawa Cancer Center under the protocol EPI-113-2018. All subjects provided written informed consent for future use of specimens for research. Experiments on animals were carried out following approval from the Kanagawa Cancer Center Animal Care and User Committee under the protocol 28-02.

PATIENT CONSENT FOR PUBLICATION

All subjects provided written informed consent for the study.

ORCID

Asami Hagiwara iD https://orcid.org/0000-0002-9713-0113

REFERENCES

1. van der Goot AT, Nollen EA. Tryptophan metabolism: entering the field of aging and age-related pathologies. *Trends Mol Med.* 2013;19:336-344.
2. Cervenka I, Agudelo LZ, Ruas JL. Kynurenines: tryptophan's metabolites in exercise, inflammation, and mental health. *Science.* 2017; 357.
3. Badawy AA. Kynurenine pathway of tryptophan metabolism: regulatory and functional aspects. *Int J Tryptophan Res.* 2017;10: 1178646917691938.
4. Platten M, Wick W, Van den Eynde BJ. Tryptophan catabolism in cancer: beyond IDO and tryptophan depletion. *Cancer Res.* 2012;72:5435-5440.
5. Uyttenhove C, Pilotte L, Theate I, et al. Evidence for a tumoral immune resistance mechanism based on tryptophan degradation by indoleamine 2,3-dioxygenase. *Nat Med.* 2003;9: 1269-1274.
6. Giusti RM, Maloney EM, Hanchard B, et al. Differential patterns of serum biomarkers of immune activation in human T-cell lymphotropic virus type I-associated myelopathy/tropical spastic paraparesis, and adult T-cell leukemia/lymphoma. *Cancer Epidemiol Biomarkers Prev.* 1996;5:699-704.
7. Suzuki Y, Suda T, Furuhashi K, et al. Increased serum kynurenine/tryptophan ratio correlates with disease progression in lung cancer. *Lung Cancer.* 2010;67:361-365.
8. Weinlich G, Murr C, Richardsen L, Winkler C, Fuchs D. Decreased serum tryptophan concentration predicts poor prognosis in malignant melanoma patients. *Dermatology.* 2007;214:8-14.
9. Schroecksnadel K, Winkler C, Fuith LC, Fuchs D. Tryptophan degradation in patients with gynecological cancer correlates with immune activation. *Cancer Lett.* 2005;223:323-329.
10. Huang A, Fuchs D, Widner B, Glover C, Henderson DC, Allen-Mersh TG. Serum tryptophan decrease correlates with immune activation and impaired quality of life in colorectal cancer. *Br J Cancer.* 2002;86:1691-1696.

11. Engin A, Gonul II, Engin AB, Karamercan A, Sepici Dincel A, Dursun A. Relationship between indoleamine 2,3-dioxygenase activity and lymphatic invasion propensity of colorectal carcinoma. *World J Gastroenterol*. 2016;22:3592-3601.

12. Miyagi Y, Higashiyama M, Gochi A, et al. Plasma free amino acid profiling of five types of cancer patients and its application for early detection. *PLoS ONE*. 2011;6:e24143.

13. Schroecksnadel K, Fiegl M, Prassl K, Winkler C, Denz HA, Fuchs D. Diminished quality of life in patients with cancer correlates with tryptophan degradation. *J Cancer Res Clin Oncol*. 2007;133:477-485.

14. Tennant TR, Kim H, Sokoloff M, Rinker-Schaeffer CW. The Dunning model. *Prostate*. 2000;43:295-302.

15. Isaacs JT, Isaacs WB, Feitz WF, Scheres J. Establishment and characterization of seven Dunning rat prostatic cancer cell lines and their use in developing methods for predicting metastatic abilities of prostatic cancers. *Prostate*. 1986;9:261-281.

16. Shimbo K, Oonuki T, Yahashi A, Hirayama K, Miyano H. Precolumn derivatization reagents for high-speed analysis of amines and amino acids in biological fluid using liquid chromatography/electrospray ionization tandem mass spectrometry. *Rapid Commun Mass Spectrom*. 2009;23:1483-1492.

17. Arashida N, Nishimoto R, Harada M, Shimbo K, Yamada N. Highly sensitive quantification for human plasma-targeted metabolomics using an amine derivatization reagent. *Anal Chim Acta*. 2017;954:77-87.

18. Gibney SM, Fagan EM, Waldron AM, O'Byrne J, Connor TJ, Harkin A. Inhibition of stress-induced hepatic tryptophan 2,3-dioxygenase exhibits antidepressant activity in an animal model of depressive behaviour. *Int J Neuropsychopharmacol*. 2014;17:917-928.

19. Kuhn DM, Ruskin B, Lovenberg W. Tryptophan hydroxylase. The role of oxygen, iron, and sulfhydryl groups as determinants of stability and catalytic activity. *J Biol Chem*. 1980;255:4137-4143.

20. Cho-Chung YS, Pitot HC. Feedback control of rat liver tryptophan pyrrolase. I. End product inhibition of trytophan pyrrolase activity. *J Biol Chem*. 1967;242:1192-1198.

21. Herr N, Bode C, Duerschmied D. The effects of serotonin in immune cells. *Front Cardiovasc Med*. 2017;4:48.

22. Aiello RJ, Bourassa PA, Zhang Q, et al. Tryptophan hydroxylase 1 inhibition impacts pulmonary vascular remodeling in two rat models of pulmonary hypertension. *J Pharmacol Exp Ther*. 2017;360:267-279.

23. Saito K, Nagamura Y, Ohta Y, Sasaki E, Ishiguro I. Characterization of the L-tryptophan transport system in the liver of growing rats. *Life Sci*. 1991;49:527-534.

24. Badawy AA. Tryptophan availability for kynurenine pathway metabolism across the life span: Control mechanisms and focus on aging, exercise, diet and nutritional supplements. *Neuropharmacology*. 2017;112:248-263.

25. Nowak EC, de Vries VC, Wasiuk A, et al. Tryptophan hydroxylase-1 regulates immune tolerance and inflammation. *J Exp Med*. 2012;209:2127-2135.

26. Franceschini B, Ceva-Grimaldi G, Russo C, Dioguardi N, Grizzi F. The complex functions of mast cells in chronic human liver diseases. *Dig Dis Sci*. 2006;51:2248-2256.

27. Cairns JA, Walls AF. Mast cell tryptase stimulates the synthesis of type I collagen in human lung fibroblasts. *J Clin Invest*. 1997;99:1313-1321.

28. Gruber BL, Kew RR, Jelaska A, et al. Human mast cells activate fibroblasts: tryptase is a fibrogenic factor stimulating collagen messenger ribonucleic acid synthesis and fibroblast chemotaxis. *J Immunol*. 1997;158:2310-2317.

29. Grizzi F, Franceschini B, Chiriva-Internati M, Liu Y, Hermonat PL, Dioguardi N. Mast cells and human hepatocellular carcinoma. *World J Gastroenterol*. 2003;9:1469-1473.

SUPPORTING INFORMATION

Additional supporting information may be found online in the Supporting Information section.